JOURNAL OF MATERIALS SCIENCE 33 (1998) 4461–4473

On the CVD of $MoSi_2$: an experimental study from the $MoCl_4$–$SiCl_4$–H_2–Ar precursor with a view to the preparation of C/$MoSi_2$/SiC and SiC/$MoSi_2$/SiC microcomposites

J. L. BOBET, G. VIGNOLES, F. LANGLAIS, R. NASLAIN
Laboratoire des Composites Thermostructuraux, UMR-47 (CNRS-SEP-UB1), Domaine universitaire, 3, allée de la Boétie, 33600-Pessac, France

The chemical vapour deposition of $MoSi_2$ on plane substrates (graphite or sintered-SiC) and ceramic fibres has been studied from $MoCl_4$–$SiCl_4$–H_2–Ar gas mixtures at $900 < T < 1400\,^{\circ}C$ and $2 < P < 40$ kPa, according to an experimental approach. $MoSi_2$ is deposited as single phase coatings for $2.5 < \alpha = P_{SiCl_4}/P_{MoCl_4} < 10$ and $10 < \beta = P_{H_2}/(P_{MoCl_4} + P_{SiCl_4}) < 20$. The deposition process appears to be thermally activated, the thermal variations of the growth rate obeying one or two Arrhenius law(s) depending on P. It seems to remain rate controlled by heterogeneous surface reactions as long as the gas flow-rate is high enough. Deposits with a smooth surface aspect and homogeneous in thickness are obtained at low T, low P and high H_2-dilution. Nicalon/$MoSi_2$/SiC and C(T300)/$MoSi_2$/SiC microcomposites are prepared and tested in tensile loading at ambient and high temperatures. They exhibit a brittle or quasi-brittle mechanical behaviour, with no (or almost no) matrix microcracking before failure. It is anticipated that dense $MoSi_2$ deposited by CVD may not be a suitable interphase material for SiC/SiC and C/SiC composite materials. © *1998 Kluwer Academic Publishers*

1. Introduction

Up to now, molydenum disilicide chemical vapour deposition (CVD) films have been used mainly as: (i) protective coatings to improve the oxidation resistance of refractory materials including molydenum itself and (ii) gates and interconnects in VLSI electronic devices [1]. These applications are related to well established properties of $MoSi_2$, namely: (i) its high thermal stability ($MoSi_2$ melts congruently at 2030 °C; (ii) its ability to form a surface oxide scale (consisting mainly of silica), when heated in an oxidizing atmosphere (e.g. air) above about 950 °C and which remains protective up to $\approx$1700 °C (as long as the oxidation regime remains itself passive); and finally (ii) its high electrical conductivity.

From a mechanical standpoint, $MoSi_2$ is brittle at room temperature as all ceramic materials. However, it exhibits a brittle/ductible transition at about 950 °C and behaves as a metal at high temperatures [2]. For all these reasons, molybdenum disilicide has been considered, more recently as a potential constituent for thermostructural composite materials eigher as a matrix [2] or as an interphase [3]. In a ceramic matrix composite (CMC), brittle fibres are embedded in a brittle ceramic matrix. CMCs exhibit the outstanding property of being tough (even though their constituents are intrisically brittle) when the fibre–matrix bonding is not too strong [4]. The fibre–matrix bonding is usually controlled through the use of an interphase material, which is a thin layer (from 0.1 to 1 m) of a compliant material predeposited on the fibre surface as a coating or formed *in situ* at the fibre–matrix interface during CMC processing. The main role of the interphase is to arrest or/and deflect the matrix microcracks which are formed under loading, thus protecting the brittle fibres from an early failure by notch effect. The most commonly used interphase material is pyrocarbon but boron nitride and noble metals (which exhibit a much higher oxidation resistance) have also been proposed [5]. $MoSi_2$, on the basis of its thermal stability, its plasticity at high temperatures and its outstanding oxidation resistance, might also be an interesting interphase material, as very recently suggested by Evans *et al.* [3].

Molybdenum disilicide can be deposited from various gaseous precursors, the most commonly cited being $SiCl_4$–$MoCl_5$–H_2 [6–9], SiH_4–$MoCl_5$–H_2 [10–12] and SiH_4–MoF_6 [13–14]. The choice of the precursor depends on the nature of the application and practical considerations. MoF_6 and SiH_4 have the advantage of being gaseous at room temperature whereas $SiCl_4$ is liquid and $MoCl_5$ solid. Thus, $MoCl_5$ has to be heated in order to achieve a high enough vapour pressure which may raise technical problems and under different the accurate control of the Mo-source gas flow-rate. The formation of stoichiometric $MoSi_2$ deposits from the SiH_4–MoF_6 precursor occurs at very low temperatures (i.e. $\approx$ 200 °C), which

might be an advantage in VLSI-technology. Conversely under such conditions the deposits are amorphous and a significant shrinkage takes place when they are further annealed for crystallization [15–16]. Finally, the use of SiH_4 as a Si-source has two drawbacks: (i) SiH_4 is a very unstable species which should be handled with care; and (ii) its reactivity is much higher than that of the Mo-sources (e.g. $MoCl_5$) with the result that silicon bearing gaseous by products can be formed, with a loss of silicon. Conversely, $SiCl_4$ exhibits a higher thermal stability.

It has been shown [17] from thermodynamic and practical considerations, that $MoCl_4$–$SiCl_4$–H_2–Ar gas mixtures are an appropriate precursor for the CVD of $MoSi_2$ (as compared to mixtures of $MoCl_5$ (or MoF_6), for the Mo-source and SiH_4 (or SiH_2Cl_2) the Si-source) [17]. Well controlled $MoCl_4$ gas flow rates can be easily achieved by chlorinating a bed of molybdenum chips with a Cl_2–Ar mixture and recording semi-continuously (with a millibalance) the weight loss of the Mo-bed (from which the $MoCl_4$ gas flow rate, $Q(MoCl_4)$, is derived). Furthermore, thermodynamic calculations have shown that the use of the $MoCl_4$–$SiCl_4$–H_2–Ar precursor has two important advantages: (i) it yields a broad, pure $MoSi_2$ deposition domain in the so-called CVD diagram (which gives the nature of the phases present in the deposit at equilibrium, as a function of the initial $MoCl_4$ and $SiCl_4$ partial pressures); and (ii) it results in higher $MoSi_2$-thermodynamic yields (i.e. up to $\approx 92\%$) with respect to the $SiCl_4$-source, for temperature/pressure conditions compatible with the chemical vapour infiltration (VCI) process [5] which would be used for depositing *in situ* a $MoSi_2$ interphase in a fibrous preform.

The aim of the present work was to establish the feasibility of the $MoSi_2$–CVD from the uncommonly used $MoCl_4$–$SiCl_4$–H_2–Ar precursor, according to an experimental approach which is complementary to the thermodynamic study [17]. More specifically, the objective of the present work was to establish: (i) the CVD parameter ranges (temperature, total pressure, gas flow rates and initial composition) compatible with the CVI process and within which $MoSi_2$ is deposited as a single phase; (ii) the relations between the $MoSi_2$ growth rate and the CVD parameters as well as those between the deposit morphology and the CVD parameters; and finally (iii) the experimental conditions under which the kinetics of $MoSi_2$ deposition are controlled by the heterogeneous surface reactions (which are those generally used in the CVI process). The results of present study were used to prepare one dimensional SiC/$MoSi_2$/SiC and C/$MoSi_2$/SiC model microcomposites in order to establish whether $MoSi_2$ could be a suitable interphase in SiC matrix reinforced with either silicon carbide or carbon fibres.

2. Experimental procedure

2.1. General considerations

The CVD of $MoSi_2$ from the $MoCl_4$–$SiCl_4$–H_2–Ar precursor, proceeds according to the following overall equation

$$2\,SiCl_4(g) + MoCl_4(g) + 6\,H_2(g) \rightarrow MoSi_2(c) + 12\,HCl(g) \quad (1)$$

with $G^{O,R}(1300\,K) = -156.2\,kJ$ and $\Delta n = 12 - 9 = 3$. The $MoCl_4$ source is formed in-line by direct chlorination at 673–923 K of a bed of molybdenum chips (contained in a superalloy or carbon curcible), with a Cl_2–Ar mixture gas flow, according to the following overall equation

$$2\,Cl_2(g) + Mo(c) \rightarrow MoCl_4(g) \quad (2)$$

with $\Delta G^{O,R}(700\,K) = -313.5\,kJ$ and $\Delta n = 1 - 2 = -1$. It has been shown [17] from thermodynamical calculations and experimental data, that pure $MoCl_4(g)$ is formed quantitatively within broad ranges of temperature and total pressure, provided the Mo chips have been first deoxidized with a pretreatment under a flow of hydrogen at 773 and 1273 K [17]. The $MoCl_4$ gas flowrate is calculated from the weight loss of the Mo chips bed, either discontinuously or semi-continuously, as explained in the next section. The flow of $SiCl_4(g)$ is generated by pumping the vapour in equilibrium with the liquid (the vapour pressure being 0.3 kPa at equilibrium at room temperature) and measured with a ball (or mass) flowmeter. Then the $MoCl_4$–Ar and $SiCl_4$–H_2 flows are mixed together inside the hot-wall deposition chamber just above the substrates to be coated.

2.2. $MoSi_2$ CVD apparatus

Two different CVD apparatuses have been used. The first (apparatus 1) was used for determining the CVD parameter ranges within which $MoSi_2$ is deposited as a single phase and for the preparation of the microcomposites. The second (apparatus 2) has been previously designed and built for the study of the deposition kinetics of refractory oxides (i.e. ZrO_2, Y_2O_3 and $ZrO_2(Y_2O_3)$) from gaseous mixtures containing metal chloride sources (i.e. $ZrCl_4$ or/and YCl_3) formed or vaporized *in situ* [18]. One of the two chlorinators has been used to form the $MoCl_4$-source.

2.2.1. Apparatus 1

The first CVD-apparatus is shown schematically in Fig. 1. The main part is a vertical silica-glass tube (diameter 50 mm), heated externally with two electrical furnaces. The upper part is the chlorination zone (heated height 220 mm) which contains the molybdenum chips bed in a superalloy crucible. The lower part is the deposition zone (height 520 mm). It is of the hot wall type and contains the substrates (usually one plane substrate of graphite or sintered SiC and a microcomposites holder). In between, a transition zone (height 120 mm) allows one to preheat the $SiCl_4$–H_2 and $MoCl_4$–Ar gas flows, on the one hand, and to control independently the temperatures of the chlorination and deposition zones, on the other hand. All the gas flowrates were measured with Rosemount

R2-15-AAA Sho-rate ball flowmeters except that of $MoCl_4$, $Q(MoCl_4)$, which was calculated at the end of the experiment from the crucible weight loss and the duration of the experiment (assuming that $Q(MoCl_4)$ was constant). The gas mixture was pumped out of the deposition zone with rotary vacuum pump through liquid nitrogentraps and the total pressure controlled with a S.A. Leybold MR16 pressure monitor. The experiments were performed with a chlorinator temperature ranging from 673 to 873 K and a deposition temperature ranging from 1173–1373 K. The total pressure was varied within the 2–40 kPa range.

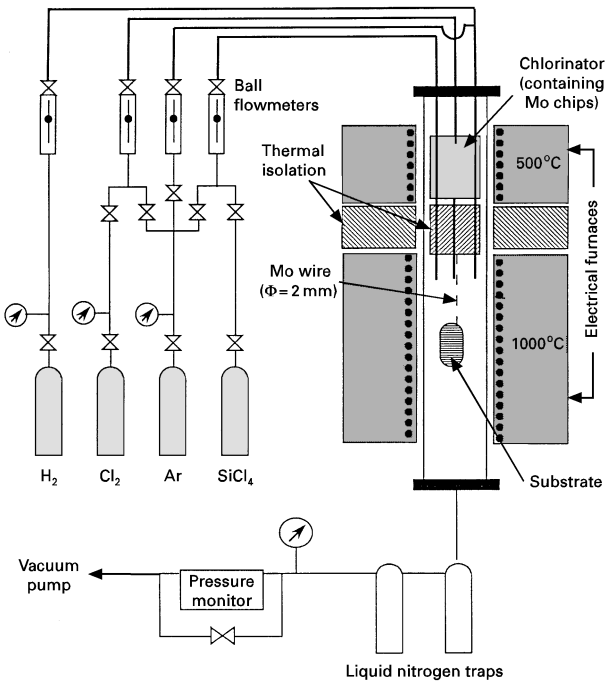

Figure 1 First apparatus used for the CVD of $MoSi_2$ (schematic).

2.2.2. Apparatus 2

The second CVD apparatus is schematically shown in Fig. 2 and has been described in details elsewhere [18]. The deposition chamber is a hot wall graphite tube (diameter 60 mm; height 350 mm). The Mo chips bed is set within a graphite crucible (diameter 40 mm; height 120 mm) just above. They are heated in dependently with r.f. coils and power supplies. The whole assembly is set inside a water-cooled stainless steel protective chamber. All the gas flow rates were measured with accurate ASM AFC 25 mass flowmeters except that of $MoCl_4$ which was calculated from the continuous recording of the weight loss of the chlorinator crucible with Mettler PM400 millibalance. Finally, the weight increase of the substrate during the CVD experiment was (with an accuracy of 2.5×10^{-6} g) is time with a Setaram B85 microbalance and used to calculate the growth rate.

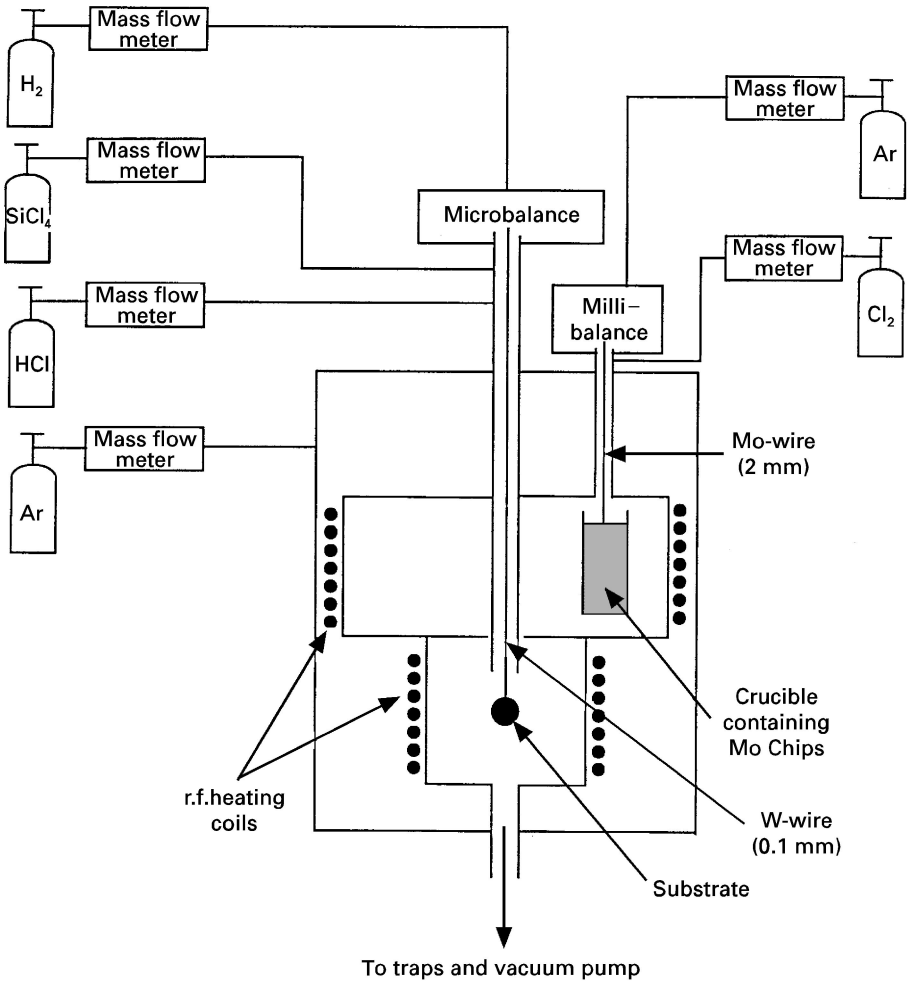

Figure 2 Second apparatus used for the CVD of $MoSi_2$ (schematic).

The experiments were performed with a chlorinator temperature ranging from 723 to 923 K and a deposition temperature ranging from 1173 to 1723 K. The total pressure was varied within the 2–40 kPa range and controlled with a MKS 252 A pressure monitor.

2.3. Substrates

To different kinds of substrate have been used in the CVD-experiments: (i) plane substrates (mainly for the growth rate measurements and effect of the CVD-parameters); and (ii) carbon Toray T300 carbon and Nicalon Si–C–O fibres (for the study of the morphology of the deposit and the preparation of the microcomposites).

Plane substrates of graphite or sintered-SiC of large size ($20 \times 20 \times 2\ mm^3$) were used for the CVD experiments performed with the first CVD unit (apparatus 1) and the X-ray diffraction (XRD) analysis of the deposits. They would be referred to as PS-1 specimens in the following. Plane substrates of smaller size either in graphite ($10 \times 5 \times 2$ or $5 \times 5 \times 2\ min^3$) or sintered-SiC (diameter 10 mm: thickness 1 mm) were used for the CVD experiments performed with the second CVD unit (apparatus 2) with a view to measure the growth rate and to assess the effect of CVD parameters on the growth rate. They would be referred to as PS-2 specimens in the following.

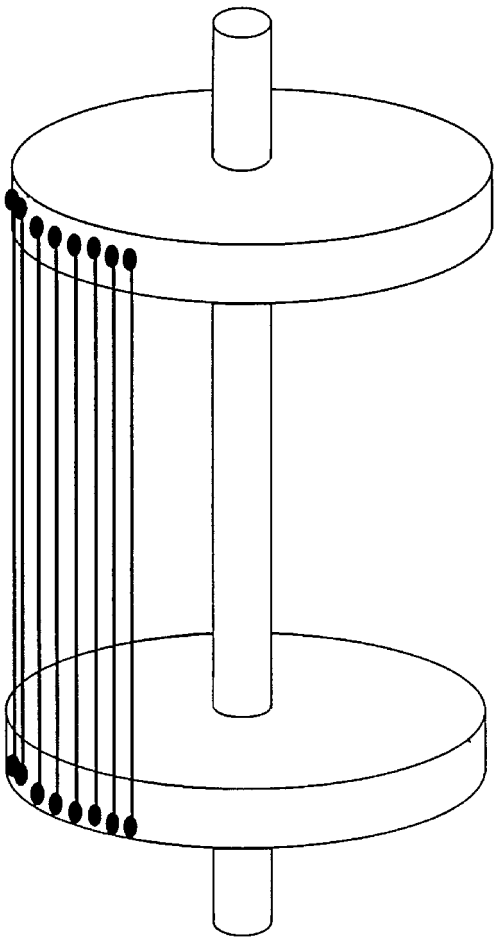

Figure 3 Barrel holder and fibre substrates used for the preparation of the C/$MoSi_2$/SiC and one-dimensional SiC/$MoSi_2$/SiC microcomposites (schematic). Capacity $\approx$80 fibres.

The fibre substrates, referred to as T300–FS or Si–C–O–FS in the following, consist of about 80 single fibres (60–80 mm in length) extracted from fibre tows and attached with a high temperature cement to a XXX barrel holder, as shown schematically in Fig. 3. These fibres were used for the preparation of the 1D-C/MoSi2/SiC and 1D-Si-C-O/MoSi2/SiC model microcomposites according to a two step CVI process: the first step being the deposition of the $MoSi_2$ interphase and the second that of SiC (which has been described in details elsewhere [19]).

2.4. Characterization

The coatings have been characterized by XRD to assess the nature of the phases and the occurrence of preferred orientations of the grains and by Auger electron spectroscopy (AES) to determine semi-quantitatively the overall chemical composition (from the intensities of the MoL_α and SiL_α transitions in the derivate $d[EN(E)]/dE$ mode spectrum and according to the peak to peak method). The morphology of the coatings deposited on the FS specimens was characterized by scanning electron microscopy.

Finally, tensile mechanical tests were performed on the as-received fibres, $MoSi_2$-coated fibres and microcomposites, either at room temperature or high temperatures, with a microtensile tester and a procedure which have been described elsewhere [20]. The failure stress data were analyzed according to the classical Weibull statistics method [21].

3. Results and discussion

3.1. Experimental conditions yielding pure $MoSi_2$ deposits

The domains of initial precursor composition (expressed in terms of initial partial pressures, P_{SiCl_4}, P_{MoCl_4} and P_{H_2} or with the $\alpha = P_{SiCl_4}/P_{MoCl_4}$ and $\beta = P_{H_2}/(P_{SiCl_4} + P_{MoCl_4})$ ratios) within which $MoSi_2$ is deposited as a single phase (i.e. free of either Mo-rich silicides of silicon) have been calculated for given temperature and pressure conditions according to a thermodynamic approach [17]. However, this approach does not take into account the kinetic factors which often play an important role in CVD, particularly at low temperatures. Thus, complementary experiments have been performed (with apparatus 1) in order to assess: (i) the range of initial composition resulting actually in pure-$MoSi_2$ deposits, for two different temperatures and pressure conditions; and (ii) the influence of temperature and pressure on the nature and porphology of the deposit.

3.1.1. Influence of the initial composition on the nature of the deposit

The influence of the initial composition of the precursor on the nature of the deposit (assessed by XRD analysis) have been studied for two temperature and pressure conditions thought to be compatible with the CVI process, namely: (i) $P = 5$ kPa; $T = 1273$ K; and

(ii) $P = 15$ kPa; $T = 1373$ K. In a first series of experiments, the partial pressures of both $SiCl_4$ and H_2 were maintained constant and that of $MoCl_4$ were allowed to vary from 0.1 to 1 kPa (and even 4 kPa in one experiment), the partial pressure of argon being adjusted in order to maintain constant the total pressure. In a second series of experiments P_{MoCl_4} were maintained constant and P_{H_2} allowed to vary. After each CVD experiment, the phases present in the deposit (PS1 specimen) were characterized by XRD. The results are shown in Tables I and II and Fig. 4a–c.

Within a given series of experiments, i.e. when the α-ratio (and correlatively the β-ratio) decreases (Table I) or increases (Table II), the nature of the deposit is observed to change in a significant manner. Initial compositions rich in $SiCl_4$ and H_2 Yield deposits consisting of $MoSi_2$ as a single phase (Fig. 4a) or even mixed with free silicon (Fig. 4b). Conversely, initial compositions rich in $MoCl_4$ result in deposits containing Mo-rich silicides (Fig. 4c) and even molybdenum itself (Table I) These results are qualitatively in good agreement with those presented earlier [17], on the basis of the thermodynamic approach (see Table I [17] Fig. 10.

TABLE I Variation of the nature of the deposit as a function of the partial pressure of $MoCl_4$ for different T, P, P_{SiCl_4} conditions (PS1-substrates)

	P_{SiCl_4}	P_{MoCl_4}	XRD results	α[a]	β[b]
	1	0.1	$MoSi_2$	10	2.7
		0.2	$MoSi_2$ + ?	5	2.5
		0.5	$MoSi_2 + Mo_5Si_3$	2	2
$T = 1273$ K		1	Mo_5Si_3	1	1.5
$P_{tot} = 5$ kPa					
$P_{H_2} = 3$ kPa	0.5	0.1	$MoSi_2$	5	5
		0.2	$MoSi_2 + Mo_5Si_3$	2.5	4.3
		0.5	Mo_5Si_3	1	3
		1	Mo_3Si	0.5	2
	1	0.1	$MoSi_2$	10	9.1
		0.5	$MoSi_2 + Mo_5Si_3$	2	6.7
		1	Mo_5Si_3 + ?	1	5
$T = 1373$ K		4	Mo_3Si + Mo	0.25	2
$P_{tot} = 15$ kPa					
$P_{H_2} = 10$ kPa	5	0.1	Si	50	2
		0.5	$MoSi_2$	10	1.8
		1	$MoSi_2$	5	1.7

[a] $\alpha = P_{SiCl_4}/P_{MoCl_4}$.
[b] $\beta = P_{H_2}/(P_{MoCl} + P_{SiCl_4})$.

TABLE II Variation of the nature of the deposit as a function of the partial pressure of $SiCl_4$ for different T, P, P_{MoCl_4} conditions (PS1 substrates)

	P_{MoCl_4}	P_{SiCl_4}	XRD results	α[a]	β[b]
	0.2	0.5	$MoSi_2 + Mo_5Si_3$	2.5	2.9
		1	$MoSi_2$	5	1.7
		2.5	$MoSi_2$ + Si	12.5	0.7
$T = 1273$ K					
$P_{tot} = 5$ kPa					
$P_{H_2} = 2$ kPa	1	0.5	Mo_3Si	0.5	1.3
		2	$MoSi_2 + Mo_5Si_3$	2	0.7
	0.5	0.1	Mo	0.2	15
$T = 1373$ K		1	$MoSi_2 + Mo_5Si_2$	2	6
$P_{tot} = 15$ kPa		5	$MoSi_2$	10	1.6
$P_{H_2} = 9$ kPa					

[a] $\alpha = P_{SiCl_4}/MoCl_4$.
[b] $\beta = P_{H_2}/(P_{MoCl_4} + P_{SiCl_4})$.

It appears from Tables I and II, that $MoSi_2$ is deposited as a single phase when the α-ratio falls between two limits, i.e. for $\alpha_i < \alpha_s$ with $\alpha_i \approx 2.5$ and $\alpha_s \approx 10$. For $\alpha \approx \alpha_i$, $MoSi_2$ is mixed with Mo-rich silicides (e.g. $MoSi_3$) and for $\alpha > \alpha_s$, it is deposited as a mixture with free silicon, as previously predicted by the thermodynamic calculations (see [17] Fig. 12).

For given temperature and pressure (e.g. $T = 1273$ K and $P = 5$ kPa) and when α is maintained constant (with a α-value resulting in a single phase $MoSi_2$-deposit, e.g. $\alpha = 5$), varying the initial hydrogen partial pressure (and thus, the value of β) does not change markedly the nature of the deposit (which remains pure $MoSi_2$), at least as long as there is enough hydrogen. Conversely, diluting the source species with hydrogen, i.e. increasing the value of β has a pronounced influence on the morphology of the $MoSi_2$-deposit, as shown in Fig. 5a, b by scanning electron microscopy (SEM). Smooth $MoSi_2$ deposits (Fig. 5a) are observed for high β-values (i.e. $\beta = 10$–20) whereas rough $MoSi_2$-deposits (Fig. 5b) are formed when β is low (i.e. $\beta = 1$–2).

Finally, the relative intensities I/I_0 of the Debye–Schener peaks observed for the $MoSi_2$ deposits (Fig. 4) are similar to those reported for $MoSi_2$-powders, suggesting that the deposits are not textured in a noticeable manner. This feature is in agreement with the pole figure study which has been reported elsewhere [22].

3.1.2. Influence of total pressure and temperature

The influence of both the total pressure and the deposition temperature on the nature of the deposit, has been studied in a new series of CVD experiments performed for $\alpha = 4$ and $\beta = 8$, (i.e. under conditions of initial composition expected to yield $MoSi_2$ single phase deposit). Total pressure and deposition temperature were varied within the range 5–50 kPa and 1273–1423 K, respectively.

The XRD analysis has shown that the deposit actually consisted of pure $MoSi_2$ whatever the values given to P and T, as expected. Furthermore, temperature was observed to have no noticeable effect on the morphology of the $MoSi_2$ deposit, at least within the temperature range studied (which is rather narrow owing to the CVI process requirement, as already mentioned). Conversely, the total pressure was found to have a significant effect on the morphology of the $MoSi_2$ deposit, as shown in Fig. 6a, b. The $MoSi_2$ coatings deposited at a given temperature (e.g. $T = 1273$ K) on a fibre substrate exhibited a rough surface aspect with many quasi-spherical nodules when formed under relatively high total pressures (Fig. 6b) and, conversely a smooth surface at lower total pressures (Fig. 6a).

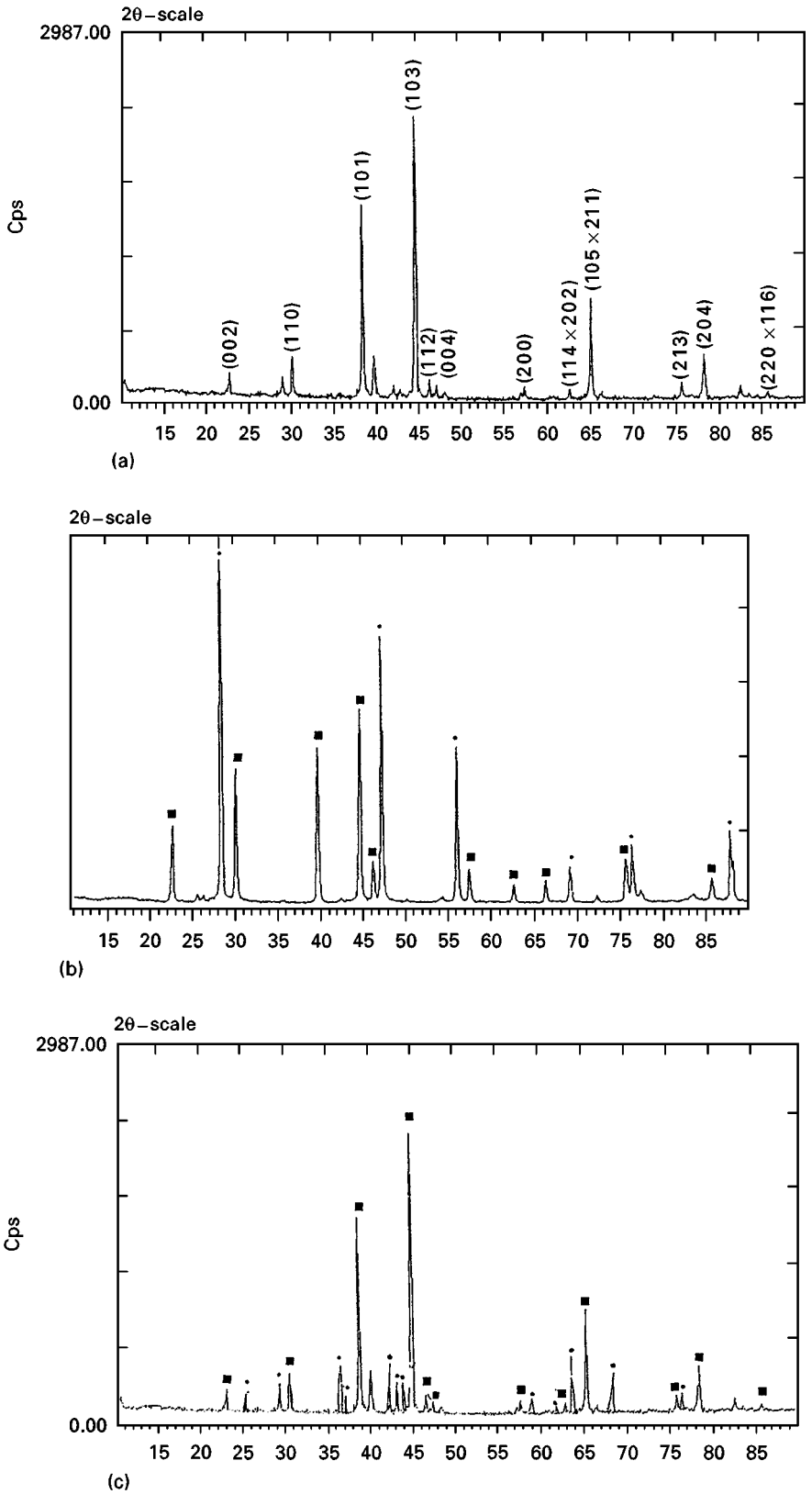

Figure 4 Debye–Scherrer patterns of $MoSi_2$-based films deposited at 1273 K and $P = 5$ kPa from $MoCl_4$–$SiCl_4$–H_2–Ar gas flows of different initial compositions: (a) single phase $MoSi_2$ deposit; (b) $MoSi_2$ (■) deposit containing free silicon (●); and (c) $MoSi_2$ (■) deposit containing Mo_5Si_3 (●) sintered SiC substrate). (a) $P_{(MoCl_4)} = 0.1$ kPa, $P_{(SiCl_4)} = 0.5$ kPa, $P_{(H_2)} = 3$ kPa, $\alpha = 5$, $\beta = 2$; (b) $P_{(MoCl_4)} = 0.2$ kPa, $P_{(SiCl_4)} = 2.5$ kPa, $P_{(H_2)} = 2$ kPa, $\alpha = 12.5$, $\beta = 0.7$; (c) $P_{(MoCl_4)} = 0.5$ kPa, $P_{(SiCl_4)} = = 1$ kPa, $P_{(H_2)} = 3$ kPa, $\alpha = 2$, $\beta = 2$.

3.1.3. Conclusion on the CVD conditions yielding single phase $MoSi_2$ deposits

From the experimental results presented above, the following main conclusions can be drawn. (i) $MoSi_2$ is deposited as a single phase deposit from the $MoCl_4$–$SiCl_4$–H_2–Ar precursor, under temperature and pressure conditions compatible with the CVI process, when $\alpha = P_{SiCl_4}/P_{MoCl_4}$ ratio falls within the range α_f–α_i (with $\alpha_f \approx 10$ and $\alpha_i \approx 2.5$); (ii) the $MoSi_2$ deposit exhibits a smooth surface aspect for high enough

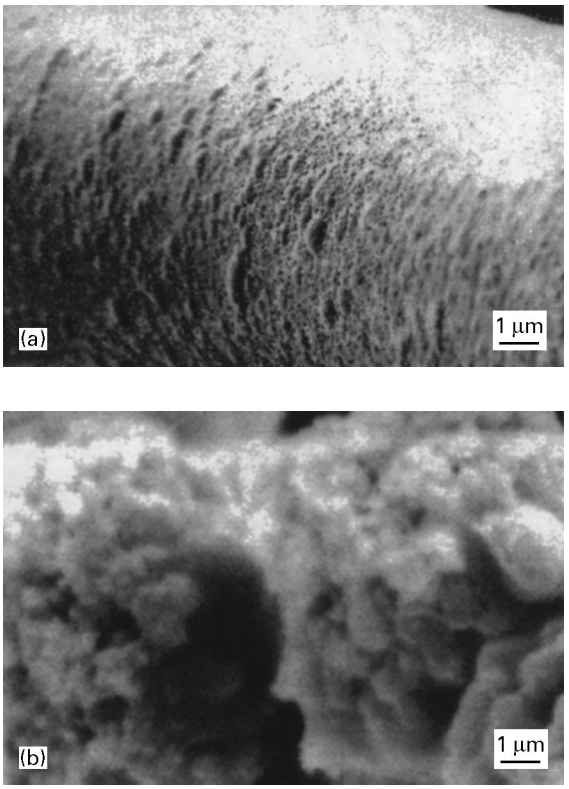

Figure 5 Morphology of $MoSi_2$ single phase films deposited on a fiber substrate at $T = 1273$ K and $P = 5$ kPa from $MoCl_4$–$SiCl_4$–H_2–Ar flow gas of different initial compositions (SEM micrography): (a) $P_{(MoCl_4)} = 0.06$ kPa $P_{(SiCl_4)} = 0.3$ kPa; $P_{H_2} = 4.6$ kPa; $\alpha = 5$ and $\beta = 12.8$ and (b) $P_{MoCl_4} = 0.2$ kPa; $P_{SiCl_4} = 1$ kPa; $P_{H_2} = 2$ kPa; $\alpha = 5$ and $\beta = 1.7$.

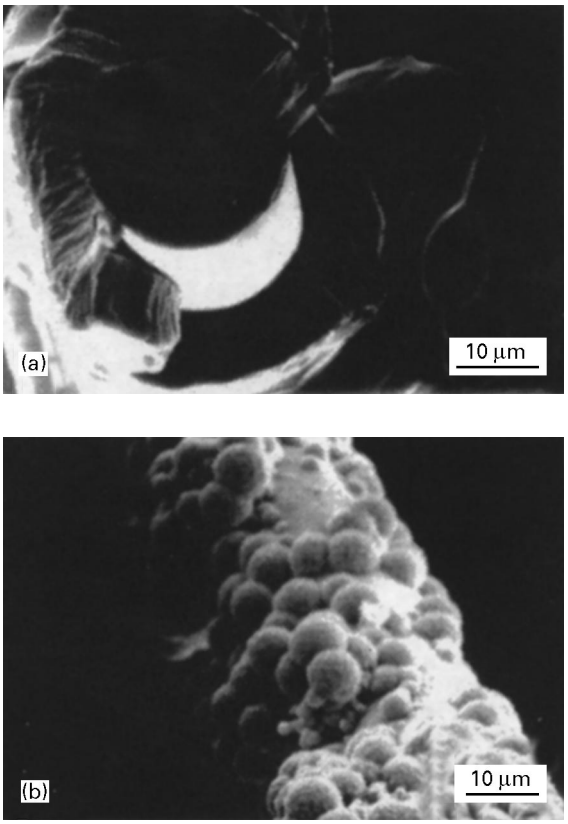

Figure 6 Morphology of $MoSi_2$ coatings deposited at $T = 1273$ K on a fibre substrate from $MoCl_4$–$SiCl_4$–H_2–Ar gas flow (with $\alpha = 4$ and $\beta = 8$: (a) at $P = 5$ kPa and (b) at $P = 15$ kPa).

values of $\beta = P_{H_2}/(P_{MoCl_4} + P_{SiCl_4})$ ratio, e.g. 10–20 and when it is formed at low total pressures. Conversely, the deposition temperature has no noticeable effect on both the composition and morphology of the deposit within the range 1273–1423 K. Thus, the following study of the growth kinetics has been performed (with apparatus 2) under conditions taking into account these main conclusions (PS2 substrates).

3.2. Influence of the CVD parameters on the kinetics of growth of $MoSi_2$ on plane substrates

3.2.1. $MoSi_2$ growth rate measurement

As already mentioned in Section 2.2, the growth rate (i.e. the mass of $MoSi_2$ deposited per unit of time and unit of substrate surface area) is derived from the continuous (or semicontinuous) recording of the specimen mass versus time, with a microbalance (apparatus 2, Fig. 2). An example of such a mass recording is shown in Fig. 7 for a sequence of three deposition experiments which have been performed successively at 900 950 and 1000 °C, all the other CVD parameters being maintained constant. In these experiments, the specimen mass has been recorded semicontinuously (with a period of 30 s). The mass–time curve exhibits three kinds of domain. The first domains, referred to as 1c, 2c and 3c correspond actually to the $MoSi_2$ deposition sequence at 900 950 and 1000 °C. Within each of these domains, the growth rate is contant and

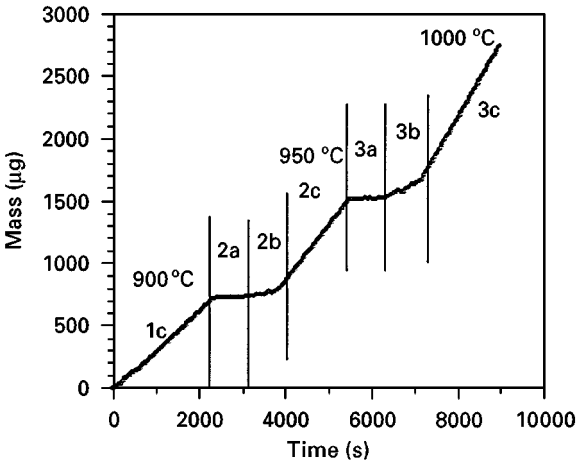

Figure 7 Semi-continuous recording of the specimen (PS2 substrate) mass variations (with a microbalance) during a sequence of $MoSi_2$ CVD experiments performed successively at 900, 950 and 1000 °C (with $P = 5$ kPa, $Q_{MoCl_4} = 4$ s.c.c.m., $Q_{SiCl_4} = 16$ s.c.c.m., $Q_{H_2} = 200$ s.c.c.m. and $Q_{Ar} = 180$ s.c.c.m.). The growth rates are calculated from the slopes of the linear segments 1 ac, 2c and 3c.

its values are calculated from the slopes of the straight lines (the slope being observed to increase as the temperature is raised, as expected). The domains referred to as 2a and 3a correspond to temperature increases, from 900 to 950 °C and 950 to 1000 °C, respectively, which require about 30 min. During these intermediate stages, the reactant gas flowrates ($Q(MoCl_4)$ $Q(SiCl_4)$ and $Q(H_2)$ were maintained at zero and there was no deposition (i.e. no mass

increase). Finally, when the substrate temperature was again stabilized the reactant gas flows were reintroduced in the deposition chamber, some time being necessary to achieve a steady state regime (domains 2b and 3b, respectively). This experimental procedure previously used for SiC [19], BN [23], ZrO_2 [18] and Y_2O_3 [18], allowed one to assess, with a limited number of experiments, the large amount of data necessary for a kinetics study.

3.2.2. Influence of temperature

The Arrhenius plots of the thermal variations of the $MoSi_2$ deposition rate are shown in Fig. 8. Within the temperature range studied (i.e. $900 < T < 1400\,^{\circ}C$) these thermal variations obey different laws depending on the value of the total pressure (with $5 < P < 40$ kPa). As low total pressures (i.e. for $P = 5$ or 10 kPa), the thermal variations of the deposition rate, $\ln R = f(1/T)$, obey two different Arrhenius laws with an apparent activation energy $E_1 = 67 \pm 4$ kJ mol^{-1} for $1173 < T < 1373$ K and $E_2 = 192 \pm 9$ kJ mol^{-1} for $1373 < T < 1673$ K, respectively. Conversely for higher total pressures, namely $P = 20$ and 40 kPa, no transition is observed in the thermal variations of the deposition rate (or it is shifted at much higher temperatures). Under such conditions, the data obey, one single Arrhenius law corresponding to an apparent activation energy $E'_1 = 63 \pm 4$ kJ mol^{-1} (i.e. similar to that reported above, for low total pressure experiments performed at low temperatures, 67 ± 4 kJ mol^{-1}). Finally, no transition towards a deposition regime controlled kinetically by transfer across the boundary layer is observed (such a transition has been reported for many CVD systems, at high temperatures). Thus, the $MoSi_2$ deposition process seems to remain controlled by heterogeneous surface phenomena within the whole temperature and all presure ranges studied. It is noteworthy that a similar conclusion has been previously drawn by Sipp in his study of the kinetics of growth of zirconia from $ZrCl_4$–CO_2–H_2–Ar precursors [18].

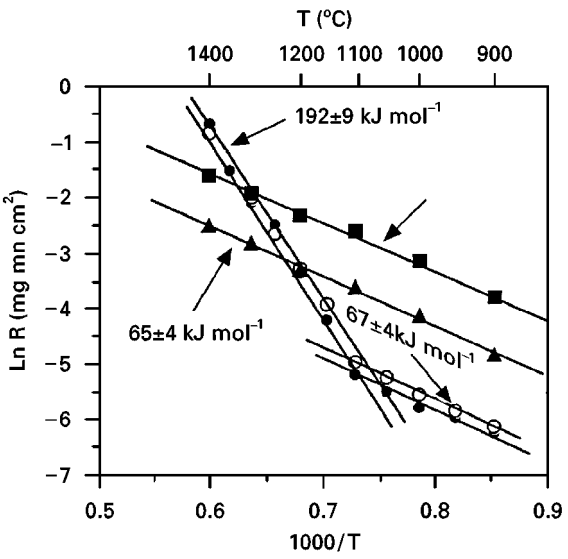

Figure 8 Arrhenius plot of the thermal variations of the $MoSi_2$ deposition rate for various total pressures (with $Q_{MoCl_4} = 4$ s.c.c.m., $Q_{SiCl_2} = 16$ s.c.c.m., $Q_{H_2} = 200$ s.c.c.m. and $Q_{Ar} = 180$ s.c.c.m). (○) 5 kPa; (●) 10 kPa; (▲) 20 kPa; (■) 40 kPa.

3.2.3. Influence of total pressure

The variations of the deposition rate of $MoSi_2$ (for $\alpha = 4$ and $\beta = 10$) as a function of the total pressure are shown in Fig. 9a, b for various temperatures within the range 900–1400 °C. The data show that there is a total pressure threshold (lying at about 10–15 kPa) beyond which the deposition rate regularly increases as P is raised. Below this threshold, the effect of the total pressure on the deposition rate is weak at low temperatures (i.e. $900 < T < 1100\,^{\circ}C$ (Fig. 9a). Conversely, it is very pronounced, for high temperatures (i.e. $1200 < T < 1400\,^{\circ}C$), the highest deposition rate being achieved at $T = 1400\,^{\circ}C$ for $P \approx 10$ kPa (Fig. 9b).

It is worthy of note that there is no total pressure domain within which R could be considered as independent of P. This feature suggests that the kinetics of growth of $MoSi_2$ remain controlled by heterogeneous chemical reactions whatever the value of P.

The data shown in Figs. 8 and 9 suggest that: (i) the kinetics of $MoSi_2$ deposition remain controlled by

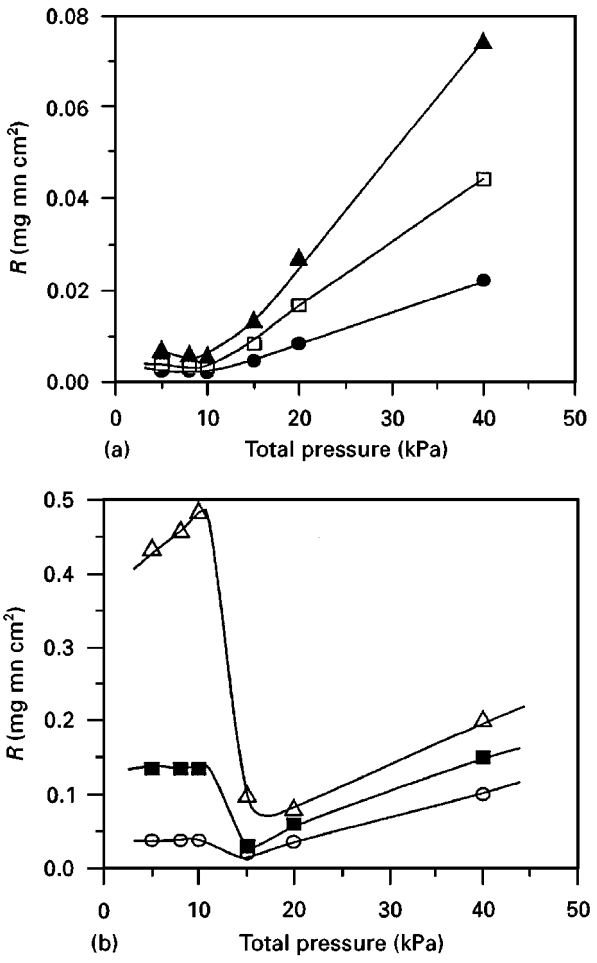

Figure 9 Variations of the $MoSi_2$ deposition rate as a function of total pressure (with $Q_{MoCl_4} = 4$ s.c.c.m., $Q_{SiCl_4} = 16$ s.c.c.m., $Q_{H_2} = 200$ s.c.c.m. and $Q_{Ar} = 180$ s.c.c.m.) for various temperatures (PS_2 specimens). (●) 900 °C; (□) 1000 °C; (▲) 1100 °C (○) 1200 °C; (■) 1300 °C; (△) 1400 °C.

chemical reactions when both T and P are varied within the ranges 900–1400 °C and 2–40 kPa, respectively; and (ii) several kinetic regimes are present. The occurrence of these regimes are shwon, schematically, in Fig. 10. In both domain A and C the apparent activation energies of the deposition process are similar and equal to about 67 kJ mol^{-1} whereas in domain B, the apparent activation energy is 192 kJ mol^{-1}, as already mentioned (see Fig. 8). In order to assess whether the deposition kinetics remain controlled by the heterogeneous surface chemical reactions (or eventually by mass transfer), a new series of experiments was performed for different total gas flow rates (PS2 specimens).

3.2.4. Influence of total gas flow rate

The variations of the $MoSi_2$ deposition rate as a function of the total gas flow rate, for CVD conditions corresponding to domains A–C, are shown in Figs 11–13. In domain A (low T and low P), no transition is observed (i.e. R seems to increase regularly as Q_{tot} is raised; (Fig. 11a). However under such conditions, the values of R are extremely low (typically of the order of 5×10^{-3} mg min^{-1} cm^{-2}) and the uncertainty considered as very large (Fig. 13). On the basis of this low dependence on Q_{tot} and of the data shown in Figs 8 and 9a, it will be assumed that the deposition of $MoSi_2$ in domain A is rate controlled by heterogeneous surface reactions.

In domains B and C a transition between two kinetic regimes is clearly observed as the total gas flow rate is raised (Figs 11b and 12). Below this transition value of Q_{tot} (i.e. for $Q_{tot} < 200$ s.c.c.m, in domain B and $Q_{tot} < 3000$ s.c.c.m. in domain C), the $MoSi_2$ deposition rate is strongly dependent on Q_{tot}, suggesting that the deposition process is rate controlled by mass transfer. Conversely, beyond this transition value, the $MoSi_2$ deposition rate is almost constant (Fig. 13) and the deposition process assumed to be kinetically controlled by heterogeneous surface reactions.

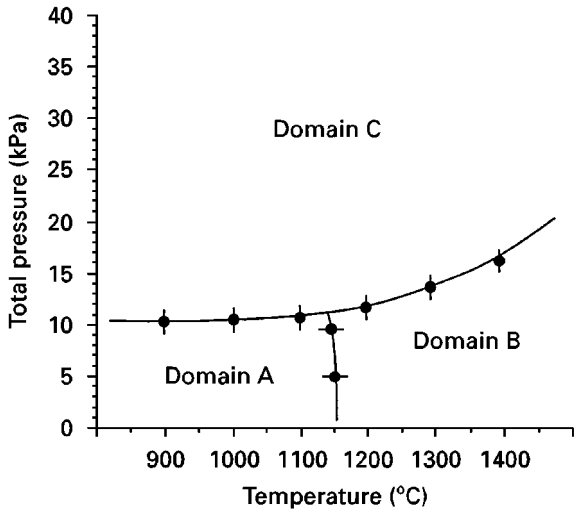

Figure 10 Kinetic $MoSi_2$ deposition domains (schematic) as drawn from the data shown in Figs 8 and 9. The CVD experiments were performed with $Q_{MoCl_4} = 4$ s.c.c.m., $Q_{SiCl_4} = 16$ s.c.c.m., $Q_{H_2} = 200$ s.c.c.m. and $Q_{Ar} = 180$ s.c.c.m.

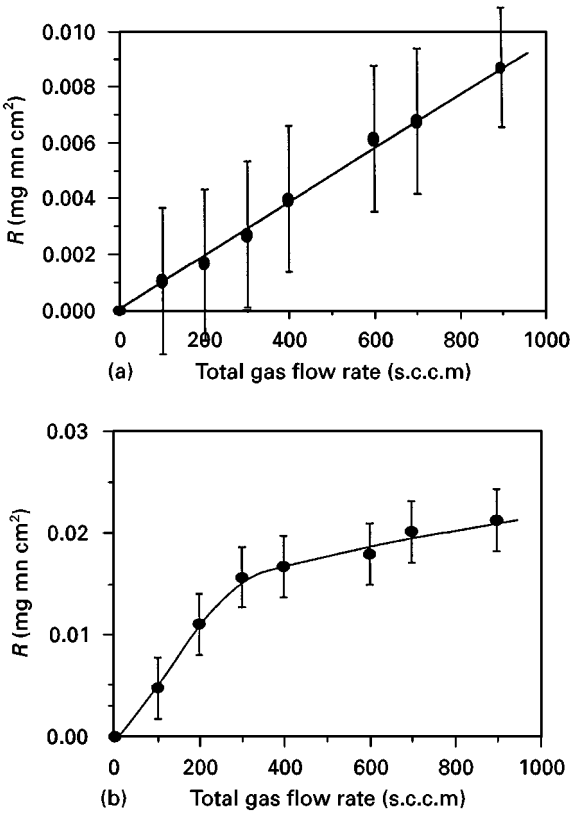

Figure 11 Variations of the $MoSi_2$ deposition rate (PS_2 specimen) as a function of the total gas flow rate at $T = 1000$ °C (with $\alpha = 4$ and $\beta = 10$): (a) for $P = 5$ kPa (domain A) and (b) for $P = 20$ kPa (domain C).

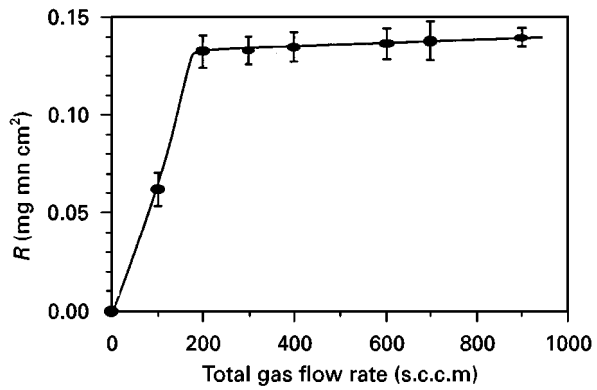

Figure 12 Variations of the $MoSi_2$-deposition rate (PS_2 specimen) as a function of the total gas flow rate at $T = 1300$ °C; $P = 5$ kPa, $\alpha = 4$ and $\beta = 10$ (domain B).

3.2.5. Conclusions of the kinetics study

The data shown in Figs 8–13 and discussed above suggest that the deposition process of $MoSi_2$ from a $MoCl_4$–$SiCl_4$–H_2–Ar gas flow remains rate controlled by the heerogeneous surface reactions, within relatively large T and P ranges, as long as the total gas fow rate is large enough.

3.3. Application to one-dimensional model microcomposites

3.3.1. CVD preparation

A microcomposite is an axisymmetrical assembly of one single fibre coated first with a thin layer of an interphase material (here $MoSi_2$) and then with the matrix (here SiC). Its mechanical behaviour in tensile loading can be considered as representative of that of actual one-dimensional CMCs when: (i) it is straight and uniform in cross-section all along its length (which supposes that both the interphase and matrix are uniform in thickness); (ii) the volume fractions are appropriate (in order to allow the matrix to undergo microcracking without an early failure of the fibre; and (iii) the fibre–matrix bonding via the interphase is similar to that in actual composites. Such requirements have been successfully achieved for both SiC/PyC/SiC and SiC/BN/SiC microcomposites. Correlations between mechanical properties and microstructural consideration are rather straight forward but the preparation and testing of such specimens should be done with care [21].

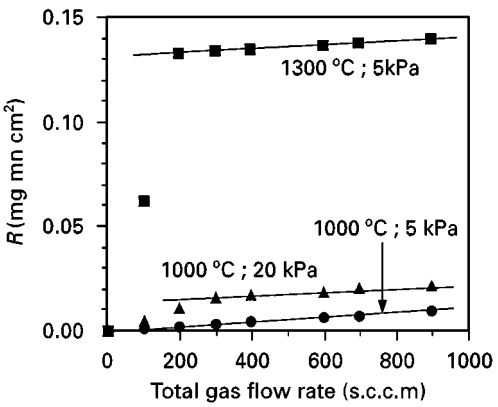

Figure 13 Variations of the $MoSi_2$ deposition rate (PS_2 specimen) as a function of the total gas flow rate drawn from the data of Figs 11 and 12 and shown to the same scale ($\alpha = 4$ and $\beta = 10$). (●) Domain A; (■) domain B; (▲) domain C.

As far as the MoS_2 potential interphase is concerned, the objective in present work was to establish, with a limited number of additional experiments, the CVD conditions yielding a $MoSi_2$ deposit on single fibres (T300 carbon fibres and Si–C–O Nicalon fibres) which should be stoichiometric, of uniform thickness along the fibre length (60 mm) and with a smooth surface aspect.

On the basis of the results presented and discussed in Section 3.1, the values of α (which controls the deposit composition) and β (which has a strong effect on the surface morphology) has been chosen as $\alpha = 4$ and $\beta \approx 10$. The remaining CVD parameters to be optimized were T, P and Q_{tot}. They varied within the following ranges. $950 < T < 1300\,^{\circ}C$; $2 < P < 20$ kPa and $100 < Q_{tot} < 400$ s.c.c.m., according to an experimental procedure using the sample holder and the CVD apparatus shown in Figs 1 and 3 and the trends drawn in the kinetics study and reported in Section 3.2.

From the results of the CVD experiments on fibre substrates (Table III) the following remarks can be made.

(i) When the temperature is raised (and whatever the total pressure), $MoSi_2$ crystals of rather large size are present in the deposit (Fig. 14a): the size of these crystals increases as the temperature is raised. These $MoSi_2$ crystals, when present in the $MoSi_2$ interphase, embrittle the microcomposites.

(ii) When, at a given temperature, the total pressure is raised, the formation of $MoSi_2$ nodules is favoured (Fig. 6b) giving a rough aspect to the $MoSi_2$ coating (whose thickness is no longer constant). This nodule formation is thought to be related to nucleation in the gas phase near the hot substrate surface (soot formation) and should be avorded (ie. by lowering the total pressure).

(iii) Under conditions of high temperature and low pressure (e.g. $T = 1300\,^{\circ}C$ and $P = 5$–10 kPa) or vice versa (e.g. $P = 20$ kPa and $T = 1100\,^{\circ}C$, the quality of

TABLE III Growth rates and morphology of $MoSi_2$ films deposited on Si–C(O) or C fibres from $MoCl_4$–$SiCl_4$–H_2–Ar

P (kPa) T (°C)	5[a]	10	20 Q_{tot} = 100 s.c.c.m.	Q_{tot} = 400 s.c.c.m.
	0.28[b]	0.26	1.2	1.5
950	VHQ; hom. MS	VHQ; hom. S	LQ numerous modules	GQ S and hom.
	0.38	0.31	1.6	1.7
1000	VHQ; hom. S	HQ but micropores S	LQ numerous modules	GQ S and hom.
	0.7	0.55	2.5	2.7
1100	GQ S (few crystals)	GQ S (few crystals)	VLQ numerous modules pores	high aspect surface non-homogeneous
Q_{tot} =	≈ 12	≈ 11	5.8	5.9
150 s.c.c.m.	VLQ rough with crystal		MQ deposit non homogeneous	
1300 Q_{tot} =	≈ 15	≈ 15	S with few modules and crystal	
400 s.c.c.m.	S (few crystals)	S but porous		

[a] Experiments with $P = 2$ kPa yield similar results

[b] Deposition rate (in μm per hour). VHQ, very high quality; GQ, good quality; MQ, moderate quality; LQ, low quality; VLQ, very low quality; S, smooth surface aspect; MS, moderately smooth; hom, homogeneous in thickness along the fibre length.

(With $\alpha = 4$ and $\beta \approx 10$) under various T–P–Q_{tot}, conditions ($Q_{tot} = 150$ s.c.c.m. unless specified and the deposition duration was 3 h.

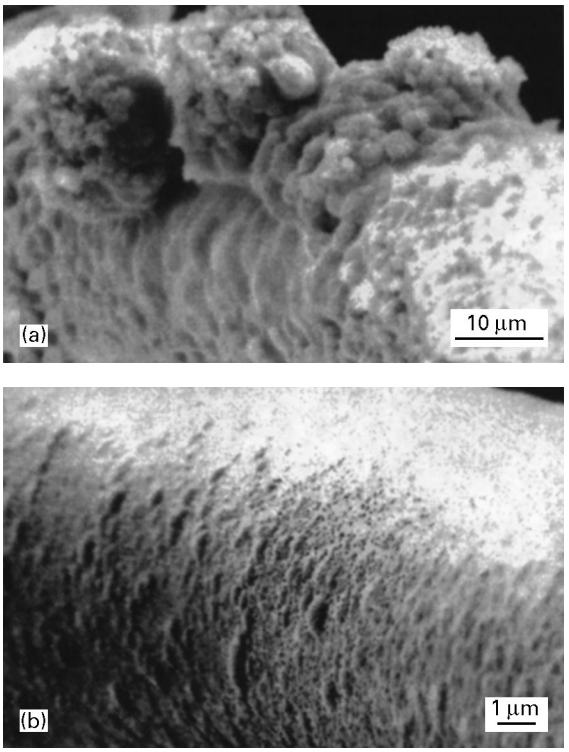

Figure 14 Morphology of $MoSi_2$ films deposited from $MoCl_4$–$SiCl_4$–H_2–Ar flow gas (with $\alpha = 4$ and $\beta = 10$) on Si–C(O) (Nicalon) fibre substrates, under various CVD conditions: (a) $T = 1573$ K; $P = 10$ kPa; $P_{(MoCl_4)} = 0.1$ kPa; $P_{(SiCl_4)} = 0.4$ kPa; $P_{(H_2)} = 5$ kPa; and (b) $T = 1273$ K; $P = 5$ kPa; $P_{(MoCl_4)} = 0.05$ kPa; $P_{(SiCl_4)} = 0.2$ kPa; $P_{(H_2)} = 2.5$ kPa.

the deposit is poor at low gas flow rates but it is improved when Q_{tot} is raised (a feature which might be related to the transition from a mass transfer rate-controlled regime to a regime kinetically controlled by surface reactions, as discussed in Section 3.2 and shown in Figs 11–13).

(iv) Under conditions of simultaneous high temperatures and high total pressures (e.g. $T = 1300\,^{\circ}C$ and $P = 20$ kPa), the quality of the deposits is moderate (smooth surface aspect with few crystals and nodules), whatever the gas flow rate. However, the deposit is strongly non-homogeneous in thickness along the fibre length. This feature is obviously related to the fact that the growth rate being high and the CVD performed in a hot wall chamber, a reactant depletion occurs along the silica tube even for high Q_{tot} values, with the result that the $MoSi_2$ thickness is much lower near the bottom of the sample holder (Fig. 3).

(v) Finally, the best $MoSi_2$ interphase coatings, in terms of surface aspect and thickness homogeneity (Figs 5a and 14b) are formed at relatively low temperature ($T < 1100\,^{\circ}C$) and pressures ($P < 5$ kPa), with a high enough gas flow rate ($Q_{tot} \approx 150$ s.c.c.m., for apparatus 1).

In a second step, the $MoSi_2$ precoated T300 or Nicalon fibre were coated, under ICVI conditions [19], with a layer of 2.5 μm of the SiC matrix.

3.3.2. Mechanical behaviour

The as-received Nicalon and T300 carbon fibres, the fibres coated with various thickness of $MoSi_2$ and the Nicalon (or T300)/$MoSi_2$/SiC microcomposites were tested in tensile loading in order (i) to study the effect of the $MoSi_2$ coating on the mechanical behaviour of the fibres and (ii) to establish whether or not the $MoSi_2$ interphase acts as "a mechanical fuse" (i.e. deflects the matrix microcracks parallel to the fibre axis in the microcomposites allowing the matrix to undergo microcracking and preventing the fibre from an early failure). The tests were performed at room temperature, except fo the microcomposites which have been tested both at ambient and high temperatures (i.e. below and beyond the brittle/ductile transition of $MoSi_2$ and the processing temperature).

3.3.3. Effect of the $MoSi_2$ coating on the fibre strength

Batches of as-received and $MoSi_2$-coated Nicalon and T300-carbon fibres were tested with a gauge length of 10 20 and 50 mm (each batch consisting of about 30 single specimens). The data were treated according to a two-parameter Weibull statistics approach in order to calculate the value of the failure stress $\sigma_{0.5}$ corresponding to a failure probability of 50% and so-called Weibull parameter *m*. Typical data are shown in Table IV (for a gauge length of $L = 25$ mm) and the corresponding Weibull plots are represented in Fig. 15.

The data show that the $MoSi_2$ film deposited on the fibre surface at about 1000 °C from the $MoCl_4$–$SiCl_4$–H_2–Ar precursor has two effects on the mechanical behaviour of the fibres. (i) It slightly reduced their Young's modulus by (9% and 14% for the Nicalon and T300 carbon fibres, respectively); and (ii) more importantly it embrittles the fibres, as supported by the decreases in fibre failure stress (i.e. 34% for Nicalon fibres and 31% for T300 carbon fibres) and Weibull modulus (50% for Nicalon fibres and 37% for T300 carbon fibres). This second feature suggests that the brittle $MoSi_2$ coating introduces new flaws on the fibres surface.

3.3.4. Microcomposite mechanical behaviour

Nicalon (or T300)/$MoSi_2$/SiC composites with $MoSi_2$ interphase thicknesses ranging from 0.15 to ≈ 1 μm and a SiC matrix thickness equal to 2 or 5 μm, were tested at 25 500 800 and 1050 °C (the latter temperature being beyond the usually accepted brittle/ductile transition of $MoSi_2$). All the specimens tested at ambient exhibited a brittle behaviour. (i.e. failure occurred within the linear elastic domain with no matrix microcracking before failure). This feature suggests that the $MoSi_2$ interphase did not act as a mechanical fuse. Similar results were also obtained for the tests performed at 500 and 800 °C.

Even when tested beyond the brittle/ductile transition of $MoSi_2$ and slightly above the processing temperature i.e. for a test temperature of 1050 °C, the microcomposites were observed to exhibit either a fully brittle (no matrix microcracking before failure) or a quasi-brittle (with statistically less than one matrix microcrack before failure) behaviours. The first

TABLE IV Tensile test and Weibull treatment data for as-received and $MoSi_2$-coated Nicalon and T300 carbon fibres (gauge length $L = 25$ mm)

	Si–C–O Nicalon fibres		T300 carbon fibres	
	As-received	$MoSi_2$-coated[a]	As-received	$MoSi_2$-coated[a]
Number of specimens	≈30	≈30	≈30	≈30
$\sigma_{0.5}$ (MPa)	2285	1377	2365	1463
$\bar{\sigma}$ (MPa)	2184	1433	2321	1592
Standard deviation	(672)	(670)	(574)	(412)
m	4.3	2.2	3.8	2.4
E (GPa)	205	187	236	202
Standard deviation	(27)	(26)	(31)	(72)

[a] $e(MoSi_2) = 0.7$ μm.

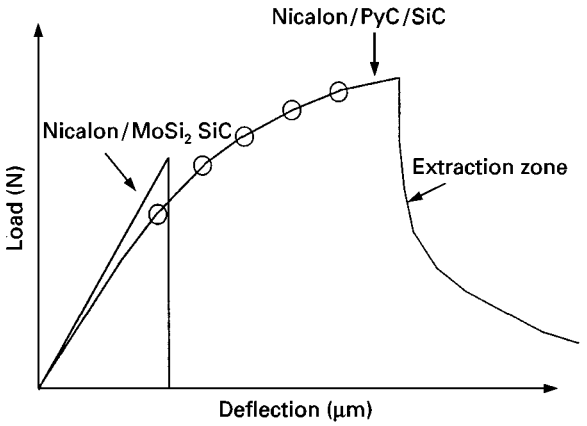

Figure 16 Schematic tensile behaviour of Nicalon/PyC/SiC [21] and Nicalon/$MoSi_2$/SiC (present work) microcomposites tested at ambient showing that the PyC interphase acts as a mechanical fuse but not the $MoSi_2$ interphase.

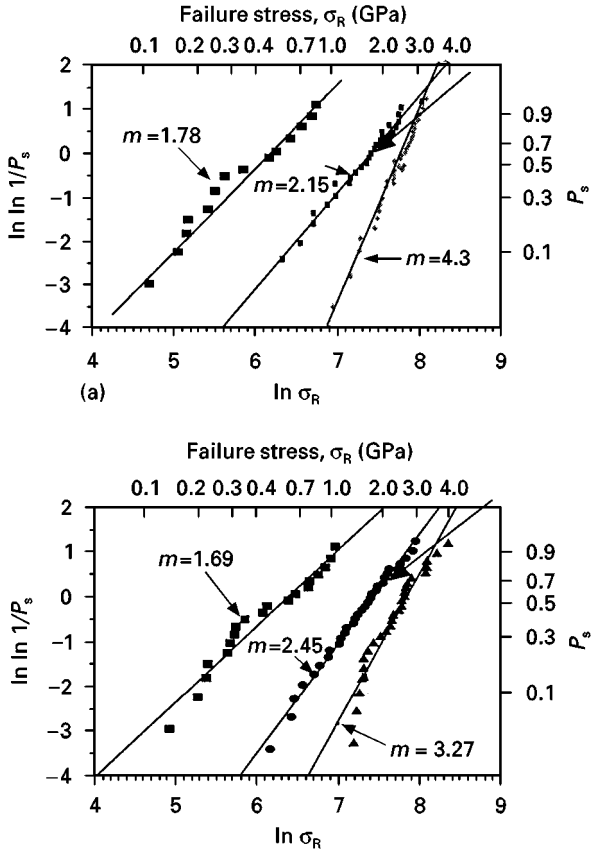

Figure 15 Weibull plots for as-received single fibres (◆), $MoSi_2$-coated single fibres (●) and related SiC–matrix microcomposites (■) drawn from ambient tensile test data (gauge length = 25 mm; $MoSi_2$ thickness = 0.7 μm, calculated Weibull parameters between ( )): (a) Nicalon fibres and (b) T300-carbon fibres.

behaviour was observed for all the T300/$MoSi_2$/SiC specimens as well as the Nicalon/MoSi2/SiC microcomposites with a thin (0.15–0.3 μm) $MoSi_2$ interphase. The second was noticed for the Nicalon/$MoSi_2$/SiC microcomposites with a thicker interphase (i.e. 0.7–1 μm).

By comparison, Nicalon/PyC/SiC and Nicalon / BN/SiC similar microcomposites were reported to exhibit up to 20 matrix microcracks (responsible for the non-linear stress–strain curve) when properly processed according to a closely related CVD/CVI technique and tested with the same apparatus as ambient (Fig. 16) [24]. It thus appears from this preliminary study that $MoSi_2$ is not a suitable interphase material for C/SiC and SiC/SiC composites, from a mechanical standpoint. This feature might be reated to (i) the high cohesion of the crystal structure of $MoSi_2$ (absence of crystallographic planes of weak debonding energy) and (ii) too strong fibre–$MoSi_2$ bonding.

4. Conclusions

From the data presented and discussed in Sections 2 and 3 the following general conclusions can be drawn.

1. $MoSi_2$ single phase coatings can be deposited from $MoCl_4$–$SiCl_4$–H_2–Ar gas mixtures as long as the $\alpha = P_{SiCl_4}/P_{MoCl_4}$ and $\beta = P_{H_2}/(P_{MoCl_4} + P_{SiCl_4})$ ratios are large enough (i.e. for $2.5 < \alpha < 10$ and $10 < \beta < 20$, either on plane graphite or sintered SiC substrates or on ceramic fibres (carbon or Nicalon fibres). Lower α-values yield deposits containing $MoSi_2$ mixed with Mo-rich silicides whereas higher α-values results in $MoSi_2 + Si$ deposits. Lower β values give deposits with a rough surface aspect.

2. The deposition of $MoSi_2$ is thermally activated within the 900–1400 °C temperature range and obeys one or two Arrhenius laws depending on the value of the total pressure. The deposition seems to remain rate-controlled by the heterogeneous surface reactions, when T and P are varied within the 900–1400 °C and 2–40 kPa ranges, as long as the total gas flow rate is high enough.

3. Nicalon/$MoSi_2$/SiC and T300/$MoSi_2$/SiC microcomposites, with a $MoSi_2$ interphase of uniform thickness and smooth surface aspects, can be prepared by deposition of $MoSi_2$ from a $MoCl_4$–$SiCl_4$–H_2–Ar gas flow ($\alpha \approx 4$ and $\beta \approx 10$) at ≈ 1000 °C and ≈ 5 kPa. These microcomposites exhibit a brittle mechanical behaviour when tested in tensile loading either at ambient or high temperatures suggesting that dense $MoSi_2$ may not be an appropriate interphase material in SiC/SiC or C/SiC composites.

Acknowledgements

This work has been supported jointly by the French Ministry of Research and SEP, through a grant given to J. L. B. The authors acknowledge the technical assistance that they received from SEP in the design of the CVD reactors (J. Rey, C. Robin-Brosse and S. Goujard) and experiments (G. Bondieu) as well as in the high temperature mechanical testing (P. Olry). They are indebted to M. Lahaye (CUMENSE) for his contribution to the AES analyses.

References

1. D. E. R. KEHR, *J. Electrochem. Soc.* **75** (1977) 511.
2. F. D. GAC and J. J. PETROVIC, *J. Amer. Ceram. Soc.* **68** (1985) C200.
3. A. G. EVANS, *J. Mater Sci.* **42** (1986) 42.
4. J. LAMON, C. RECHINIAC, N. LISSART and P. CORNE in: Proceedings of the 5th ECCM, edited by A. R. Bunsell *et al*., (EACM, Bordeaux, 1992) p. 895.
5. M. HANNACHE, F. LANGLAIS and R. NASLAIN *J. Less. Common Metals* **95** (1983) 221.
6. S. MOTOJIMA and H. YOSHIDA, *J. Mater. Sci. Lett.* **1** (1982) 23.
7. *Idem. ibid.* **1** (1989) 1323.
8. Y. MEMROMTRA and N. S. STOLOFF, Materials Technology Corporation (unpublished).
9. C. H. REYNOLDS, DARPA/ONR Program, Review (1990).
10. S. INOUE, N. TOYOKURA, T. NAKAMURA, *J. Electrochem. Soc.* (1983) **44** 1603.
11. S. INOUE and T. NAKAMURA, *Thin Solid Films* **173** (1989) 235.
12. D. E. R. KEHR, "Chemical vapor deposition of $MoSi_2$" (The Electrochemical Society, Princeton, NJ, 1977).
13. G. A. WEST and K. W. BEESON, *J. Electrochem. Soc.* **135** (1988) 1752.
14. P. J. GACZI, *ibid.* **8** (1987) 32.
15. D. E. R. KEHR, in Proceedings of the 6th International Conferences on CVD, **75** (1977) p. 511.
16. O. UNAL and J. J. PETROVIC, *J. Amer. Ceram. Soc.* **73** (1990) 1752.
17. J.-L. BOBET, R. NASLAIN and C. BERNARD, *Journal of Chemical Vapor Deposition* **3** [3] (1996) 223.
18. E. SIPP, Thesis n°483, University of Bordeaux, Bordeaux (1990).
19. F. LANGLAIS and C. PREBENDE, in Proceedings of the 11th International Conference on CVD, edited by K. E. Spear and G. W. Cullen pp. 686–695 (Electrochemical Society Pennington, NJ, 1990) p. 686.
20. J. L. BOBET, Thesis n°987, University of Bodeaux, Bordeaux (1993).
21. J. LAMON and N. LISSART in Proceedings of the 17th Annual Conference on Composites and Advanced Ceramics, Coco Beach, FL (American Ceramic Society).
22. J.-L. BOBET, A. GUETTE, R. NASLAIN, N. JI and J.-L. LEBRUN, *Acta Metall Mater* **43** [6] (1995) 2255.
23. S. PROUHET, F. LANGLAIS, A. GUETTE, R. NASLAIN and J. REY, *Eur. J. Solid State Inorg. Chem.* **30** (1993) 953.
24. F. REBILLAT, Internal LCTS report (1992).

Received 23 October 1995
and accepted 24 April 1996